Pharmacogn. Mag.
A multifaceted peer reviewed journal in the field of Pharmacognosy and Natural Products
www.phcog.com | www.phcog.net

ORIGINAL ARTICLE

Application of Sodium Alginate and Chitosan for Compound Volatile Oils From *Rimulus cinnamon* and *Angelica sinensis*: Microcapsules Preparation, Evaluation, Characterization, and *in vitro* Release Study

Wensheng Lai[1], Yanling Liu[1], Yanhui Kuang[2], Sisi Zhang[2], Chuanping Zhang[2], Chuyuan Li[2], Bohong Guo[1]

[1]Department of Pharmaceutics, School of Pharmacy, Guangdong Pharmaceutical University, Guangzhou, [2]Guangzhou Baiyun Mountain and Hutchison Whampoa Ltd., Modern Chinese Medicine Research Institute, Guangzhou, China

Submitted: 26-Mar-2022 Revised: 10-May-2022 Accepted: 01-Aug-2022 Published: 23-Nov-2022

ABSTRACT

Background: The compound volatile oils (CVOs) from *Rimulus cinnamon* and *Angelica sinensis* are commonly used together in many compounds. The unstable and volatile nature of CVOs limits their application. **Objectives:** The objective of this study was to prepare and evaluate the CVOs microcapsules. **Materials and Methods:** Chitosan (CS) and sodium alginate (SA) were used as composite wall materials to encapsulate CVOs using the complex coagulation method. The microcapsules were characterized by scanning electron microscopy (SEM), Fourier transforms infrared spectroscopy (FT-IR), X-ray diffraction (XRD), and thermogravimetric (TG). The drug loading (DL%), encapsulation efficiency (EE%), *in vitro* release behavior, and stability of the microcapsules were studied. **Results:** DL (%) and EE (%) of microcapsules were 22.60 ± 0.02% and 72.55 ± 0.04%, respectively. SEM showed that microcapsules were spherical and the surface was not smooth, with lump-like folds, minor dents, and cracks. FT-IR and XRD confirmed the inclusion of CVOs within microcapsules. TG analyses indicated that the microcapsules possess strong heat resistance. Swelling experiments reflected the response of microcapsules to different pH values. Swelling ratios in acidic, neutral, and alkaline media were 2.47 ± 0.07, 1.75 ± 0.03, and 1.04 ± 0.01, respectively. The *in vitro* release behavior of the CVOs microcapsules demonstrated a sustained release property. Furthermore, the microcapsules had excellent stability, and the DL was 15.12% after storage at 25°C for 60 days. **Conclusion:** The CVOs microcapsules prepared by SA and CS not only showed regular appearance, uniform particle size, responsiveness to different pH values, and sustained release properties *in vitro* but also exhibited good DL performance and stability, which was helpful for further development into the various specific formulation.

Key words: Chitosan, complex coagulation, compound volatile oils, microcapsule, sodium alginate

SUMMARY

- The CVOs were successfully microencapsulated and demonstrated to have good drug loading properties and stability. In the follow-up research, it will be further formed into specific dosage forms to expand the scope of application.

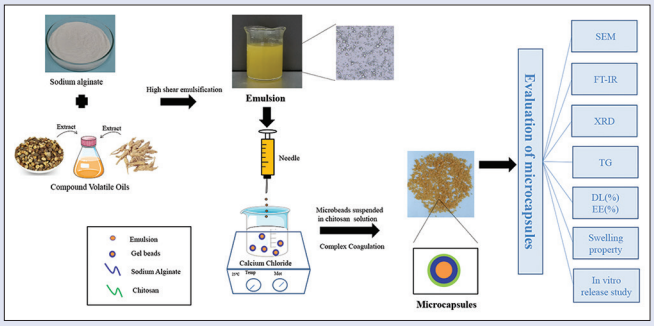

Abbreviations used:
CVOs: Compound volatile oils; CS: Chitosan; SA: Sodium alginate; SEM: Scanning electron microscopy; FT-IR: Fourier transform infrared spectroscopy; XRD: X-ray diffraction; TG: Thermogravimetric; DL %: Drug loading; EE %: encapsulation efficiency; $CaCl_2$: Calcium chloride; GC-MS: Gas Chromatography-Mass Spectrometer; SGF: Simulated gastric fluid; NS: Normal saline; SIF: Simulated intestinal fluid; O/W: Oil-in-water.

Correspondence:
Dr. Bohong Guo,
Department of Pharmaceutics, School of Pharmacy, Guangdong Pharmaceutical University, 280 East Waihuan Road, Guangzhou Higher Education Mega Center, Guangzhou - 510006, China.
E-mail: guobohong@gdpu.edu.cn
DOI: 10.4103/pm.pm_129_22

Access this article online
Website: www.phcog.com
Quick Response Code:

INTRODUCTION

Rimulus cinnamon, the dry shoot of *Cinnamomum cassia* Presl, is commonly used to treat phlegm, amenorrhea, cold, and heart palpitations.[1] In traditional clinical practice, *R. cinnamon* has the effect of sweating and relieving muscles, warming meridians and dispelling cold, correcting the disharmony between the camp and the guard, relieving the wind evil, and subsidizing the internal organs.[2] Modern pharmacological studies of traditional Chinese medicine point out that cinnamon also has anti-tumor, anti-inflammation, bacteriostatic, immune-enhancing, anti-oxidation, and proliferation-regulating functions.[3] *Angelica sinensis*, the dried root of the *Umbelliferae Angelica sinensis* (Oliv.) Diels, mainly has the effect of invigorating blood circulation, regulating menstruation, and relieving pain, as well as moistening intestines and defecating.[4] In many compounds, *R. cinnamon* and Angelica are commonly used together.[5,6] Guanxin

Cite this article as: Lai W, Liu Y, Kuang Y, Zhang S, Zhang C, Li C, *et al*. Application of sodium alginate and chitosan for compound volatile oils from *Rimulus cinnamon* and *Angelica sinensis*: Microcapsules preparation, evaluation, characterization, and *in vitro* release study. Phcog Mag 2022;18:1045-54.

Kang capsule prescription, which contains Angelica and *R. cinnamon*, has vessel-unblocking, heart-benefiting, kidney-strengthening, and stasis-dissipating effects.[7] It is often used to treat coronary heart diseases. Yukui capsules, a traditional Chinese medicine compound used for the treatment of peptic ulcers with deficiency and colds of the spleen and stomach, have the effects of replenishing vitality, promoting blood circulation, warming the spleen and stomach, suppressing soreness, clearing meridian and relieving pain.[8] Modern pharmacological experiments prove that the classic Danggui Sini Decoction has the effect of treating cardiovascular and cerebrovascular diseases.[9] In the sovereign drugs *R. cinnamon* and *A. sinensis*, the main components of the compound volatile oils (CVOs) easily volatilize during preparation, which will inevitably reduce the effectiveness of the decoction.[10] To improve its stability, β-cyclodextrin is often used for inclusion to make a stable powder.[11] However, the water solubility of β-cyclodextrin is as low as 1.85% at room temperature. Moreover, the preparation process requires a large number of cyclodextrin materials and thereby severely limiting its clinical application. Therefore, CVOs were microencapsulated to solve the limitation of the volatile oil inclusion compound, increase the drug loading (DL) rate of volatile oil, and expand its application.

Microcapsule refers to the tiny capsule (1 ~ 250 μm) formed by wrapping gaseous, liquid, or solid drugs in natural or synthetic polymer materials.[12] Microencapsulation of drugs is one of the important directions in the study of new dosage forms of modern drugs. It can solve some problems such as easy oxidation, volatile, incompatibility, poor absorption, and quick release in the preparation process.[13] With the microencapsulation technology, liquid or gas solidification can be realized to slow down the loss of volatile core material as well as the isolation and protection of active ingredients, improve the stability of the core material, and decelerate and control its release.[14,15] Microencapsulated drugs are available in different dosage forms, such as powder, tablet, granule, capsule, and injection. Chitosan (CS) and sodium alginate (SA) are widely used as wall materials for the preparation of microcapsules owing to their non-toxicity and high biodegradability.[16] The main direction of current research is to treat the volatile oils with a composite wall material for encapsulation, which will achieve the slow and controlled drug release or to powder the volatile oils.[17,18] CS, a natural alkaline cationic polysaccharide, is prepared by removing a part of the acetyl group of chitin.[19,20] N-glucan and N-acetylglucan are the structural units in the molecular chain of CS.[21] CS has the advantages of good biocompatibility, biodegradation by a variety of enzymes in the body, non-toxicity, non-antigenicity, abundant resources, and low cost. At the same time, CS has unique molecular structure characteristics, chemical properties, and biological functions. CS has become a polymer biomaterial widely used in biomedicine and other fields. SA, a natural linear anionic polysaccharide, is formed from the sodium salts of α-L-arosuronic acid and β-D-mannouronic acid by α (1-4) glycosidic bond.[22] SA is easily soluble in water, but insoluble in ethanol, ether, chloroform, and acids with a pH lower than that. SA has good stability, thickening, film-forming, chelating, and flocculating properties.

The reaction mechanism of SA-CS microcapsules prepared by complex coagulation is shown below. First, an SA solution was dropped into a calcium chloride ($CaCl_2$) solution, and then the sodium ions in the SA and the calcium ions in the $CaCl_2$ solution were exchanged, forming calcium alginate gel beads with certain mechanical strength and elasticity through the calcification reaction.[23,24] The calcium alginate gel beads were transferred to a complex coagulation reaction in CS solution. Then, complex coacervation between the abundant negatively charged carboxyl groups in SA and the positively charged amino groups on the side chain of CS formed close polyelectrolyte composite membranes.[25] In this study, CS and SA were used as composite capsule materials to encapsulate CVOs and investigate the appearance, particle size, encapsulation efficiency (EE %), DL (%), stability, and *in vitro* release trend of microcapsules.

MATERIALS AND METHODS

Materials

CVOs were extracted from *R. cinnamon* and *A. sinensis* (mixing ratio 1:1, *v/v*; each gram of the mixed volatile oil contains 0.53 g of cinnamaldehyde) and were obtained from Jingjing Biotechnology Co. Ltd. (Guangzhou, China). SA was purchased from Qingdao Mingyue Seaweed Group Co. Ltd. (Shandong, China). CS (85% deacetylation degree) was purchased from Shandong Aokang Biotechnology Co. Ltd. (Shandong, China). Methanol and acetonitrile (HPLC grade) were purchased from Beijing Dikma Technology Co., Ltd. (Beijing, China). All other chemicals were of analytical grade and obtained commercially.

Identification of CVO

CVOs were determined by gas chromatography coupled with mass spectrometry (GC-MS). The analysis was performed on a GC-MS 7890B-5977A (Agilent Technologies, Santa Clara, CA, United States) with an HP-5MS column of 60 m × 250 μm × 1.4 μm (Agilent Technologies, Santa Clara, CA, United States) and helium as carrier gas with a flow rate of 0.43 mL/min. For sample heating, the column temperature was maintained at 70°C for 3 min and then increased to 250°C, at 3.5°C/min, and kept for 10 min.

Preparation of CVOs microcapsules

SA solutions at different concentrations (0.50%, 1.0%, and 1.5%) were each mixed with CVOs and stirred evenly. Emulsions were formed under high-speed shear for 5 min at the speed of 10,000 $r \cdot min^{-1}$ with a digital high-speed disperser (T25, IKA, Germany). Then, an emulsion was dropped slowly into the $CaCl_2$ solution to form calcium alginate gel beads. After that, the beads were dispersed in a CS solution and coagulated for 2 h to form microcapsules. After filtration, the resulting microcapsules were washed with petroleum ether three times and vacuum-dried at 40°C for 12 h. The main mechanism of CVOs loaded into microcapsules is as follows: the CVOs were emulsified in SA solution and then gradually dropped into calcium chloride solution. The sodium ions in the SA exchanged with the calcium ions in the calcium chloride solution, and the calcium alginate gel particles with certain mechanical strength and elasticity were formed through the calcification reaction. Finally, the calcium alginate beads were transferred to the CS solution for a complex coagulation reaction. A large number of positively charged primary amino groups in the side chain structure of CS and a large number of negatively charged carboxyl groups in the SA structure can undergo complexation reactions through anion and cation attraction to form a tight polyelectrolyte composite membrane.

Analysis of DL (%) and EE (%) of CVO microcapsules using HPLC

The content of cinnamaldehyde was determined as the basis to identify the amount of DL (%) and EE (%) of the CVO microcapsule. The microcapsules were placed into a volumetric flask with a small amount of distilled water and placed overnight to fully expand the capsule material.[26] Then, a certain amount of ethanol was added, followed by an ultrasound for 30 min and ethanol was used for constant volume. After filtration, the filtrate was diluted appropriately, and the content of cinnamaldehyde in microcapsules was determined by the HPLC system (Essential LC-15, SHIMADZU, Japan). Chromatographic separation was carried out on a C_{18} column (250 mm × 4.6 mm, 5 μm, Dikma Technologies, China).

The mobile phase was acetonitrile: water (40: 60) and the flow rate was 1.0 mL/min at 30°C.

Percentage DL and EE of CVOs microcapsules were determined according to Eqs. (1) and (2):

$$DL(\%) = \frac{\text{Amount of cinnamaldehyde in microcapsules}}{\text{The mass of microcapsules sample}} \times 100\% \quad (1)$$

$$EE(\%) = \frac{\text{Amount of cinnamaldehyde in microcapsules}}{\text{Theoretical amount of cinnamaldehyde in microcapsules}} \times 100\% \quad (2)$$

Characterization of CVO microcapsules

Morphology of emulsion

The microscope (DM3000 LED, Leica, Germany) was used to observe the morphology of the emulsion, which was prepared with different concentrations of SA.

SEM analysis

The morphology of the CVOs microcapsule was analyzed using a scanning electronic microscope (sigma500, Zeiss) with an extra high tension of 10.00 kV.

FT-IR analysis

The CVOs, SA, CS, blank microcapsules, physical mixture, and microcapsules were performed with a Fourier Transform Infrared spectrometer (Spectrum100, Perkin Elmer), from 4000 to 400 cm^{-1}, using the KBr disc method.

XRD analysis

XRD measurement was performed by using an X-ray diffraction instrument (D8 Adance-Bruker, Germany) to analyze SA, CS, blank microcapsules, microcapsules, and physical mixture with the 2θ range from 10° to 50°.

TG

The thermal stability of capsule material and the microcapsules was determined by thermogravimetric analysis (TGA) using TGA 209F1 Libra (Corporation NETZSCH, Germany). The analysis was conducted under the following operating conditions: alumina pan; dynamic nitrogen atmosphere with the flow of 20 mL/min; heating rate: 10°C min^{-1}, temperature range: 35°C to 600°C.

Swelling studies

The swelling degree of microcapsules was assessed using a modified method described by Chaib *et al.* (2021)[27] A certain amount of microcapsules were accurately weighed and submerged in 20 mL simulated gastric fluid (SGF), normal saline (NS), and simulated intestinal fluid (SIF) at 37°C. Microcapsules were taken out at 0, 20, 40, 60, 90, and 120 min and the swelling ratio was expressed as the percentage of diameter changed according to the following Eq.-(3):

$$\text{Swelling ratio} = \frac{p_i}{p_0} \quad (3)$$

Where P_i is the average diameter of microcapsules at the ith sampling time point and P_0 is the initial diameter of microcapsules.

In vitro release study

A certain amount of CVOs microcapsules were accurately weighed and placed in 900 mL of SGF, NS, and SIF, respectively. The dissolution rate was evaluated by the rotary basket method using the ZRS-8G intelligent dissolution tester at a rotating speed of 50 rpm and the temperature was maintained at 37 ± 0.5°C. At different time points (0.25, 0.5, 0.75, 1, 1.25, 1.5, 2, 2.5, 3, 4, and 6 h), 2 mL test solution was taken out. The test solution was detected by the HPLC system and an equivalent volume of corresponding fresh dissolution media was added. Similarly, physical mixtures were added directly to the same medium to investigate the release behaviors difference between physical mixtures and microcapsules.

Percentage cumulative release rate (Q) of CVOs microcapsules was determined according to Eq. -(4):

$$Q = \frac{C_n \cdot V + \sum_{i=1}^{n} C_i \cdot V_i}{W \times DL} \times 100\% \quad (4)$$

where W is the total mass of the microcapsules (g); DL is the drug loading of the microcapsule, and Cn is the drug concentration of the sample at the nth sampling time point ($mg \cdot ml^{-1}$); Ci represents the drug concentration taken at the ith sampling time point ($mg \cdot ml^{-1}$); V represents the total volume of the dissolution medium (ml), and Vi represents the sampling volume at the ith sampling time point (ml).

Drug release kinetics

The kinetics of drug release was studied by applying four different kinetic models namely, zero order, first order, Ritger-Peppas, and Higuchi models.[28] The kinetic model was determined by comparing the curve fitting method and their correlation coefficient values. The formula used to fit the release curve is as follows:

Zero-order: $Q = K_0 t$ (5)

First-order: $\ln(1 - Q) = K_1 t$ (6)

Higuchi: $Q = K_H t^{1/2}$ (7)

Ritger-Peppas: $Q = K_m t^n$ (8)

Q: is the cumulative amount of drug released at time t; t: is the time in minutes; Km: is the kinetic constant; K_H: is Higuchi constant; Ko: is zero-order release constant; K_1: is first-order release constant; n: is the diffusion or release exponent of Ritger-Peppas order.

Storage stability study

The microcapsules and physical mixtures were placed in a constant temperature and humidity test chamber (temperature of 25°C, relative humidity of 75%). The change of DL (%) was measured over 90 days.

Statistical analysis

All experiments were performed in triplicate as independent experiments and data were expressed as mean values ± the standard deviation (SD). Analysis of variance (ANOVA) was assessed with SPSS 22.0 (SPSS Inc., Chicago, IL). The statistical difference was determined at a 95% confidence level.

RESULTS AND DISCUSSION

GC-MS analysis of CVOs

The chemical composition of CVOs was qualitatively and quantitatively analyzed by gas chromatography-mass spectrometry (GC-MS). Totally 28 compounds were identified [Table 1]. The GC-MS total ion flow diagram of CVOs was shown in Figure 1. The main constituents of the examined essential oils are cinnamaldehyde (55.75%), trans-ligustilide (36.23%), dibutyl phthalate (1.92%), and 1(3H)-isobenzofuranone, 3-butylidene (1.22%). Cinnamaldehyde is the main component and thus is used as an index to evaluate the DL (%) and EE (%) of CVOs microcapsules.

DL (%) and EE (%) of CVOs microcapsules

The formulation of microcapsules depends on many factors, such as the concentrations of SA, CS, and $CaCl_2$. The effects of SA concentration

on DL (%) and EE (%) are presented in Table 2. The DL (%) and EE (%) generally increase as the SA concentration rises from 0.5% to 1.0% [Table 2]. The DL (%) and EE (%) reach 22.60 ± 0.02% and 72.55 ± 0.04%, when the SA concentration is 1.0%. The reason is that the SA solution at a higher concentration provides more sodium ions from the α-L-guluronic acid to exchange with Ca^{2+}, forming cross-linked network structure of calcium alginate gels.[29] However, too high an SA concentration (1.5%) will reduce the physical properties of the microspheres, such as smoothness, thus affecting the microsphere performance. As reported similarly, high-concentration SA possesses high viscosity, leading to lower EE.[30] The SA concentration greatly influences the formability of the microcapsules.[31,32] As shown in Figure 2, SA and CVOs at different concentrations can form round and regular oil-in-water (O/W) emulsions. However, the thickness and strength of the emulsions are not excellent for the low charge density when the SA concentration is low (0.5%) [Figure 2a].[33] The amount of O/W emulsions as obtained is relatively small. When the SA concentration is 1.0%, the emulsions are regularly spherical and well dispersed with a uniform shape and size [Figure 2b] and a smooth surface. When the SA concentration is 1.5%, more spherical emulsions can be obtained [Figure 2c]. At higher SA concentration, the viscosity of the continuous phase increases. Under stirring, the dispersion degree of materials is reduced due to greater resistance.[34]

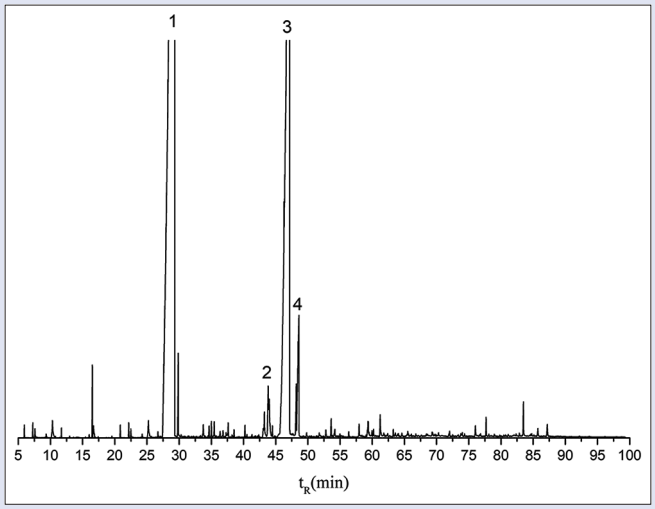

Figure 1: The GC-MS total ion flow diagram of the compound volatile oil. Peak identity: 1, cinnamaldehyde, (E)-; 2, 1 (3H)-Isobenzofuranone, 3-butylidene; 3, trans-ligustilide; 4, dibutyl phthalate

In previous research, microcapsules were prepared using 1.0%, 2.0%, and 3.0% $CaCl_2$ solutions and DL (%) and EE (%) were determined. When the $CaCl_2$ concentration was increased from 1.0% to 2.0%, the DL (%) of the microcapsules showed little difference. When the $CaCl_2$ concentration rises to 3.0%, both DL (%) and EE (%) decrease significantly. Gelation along with cross-linking of SA is achieved by the exchange of sodium ions from the α-L-guluronic acid with Ca^{2+} to form a characteristic egg-box-like structure.[35,36] At low $CaCl_2$ concentration, most of the $CaCl_2$ is absorbed by the bulk SA, but at high $CaCl_2$ concentration, bulk cross-linking and microcapsule surface cross-linking can take place simultaneously with partial penetration into the alginate droplets to produce a moderately solidified surface layer. When the cross-linking density per unit volume is high

Table 1: Chemical composition of the compound essential oil

R.T. (min)	Identified compound	Sourc	Content (%)
5.582	Propanoic acid, ethyl ester	R.C	0.269
16.504	trans-β-Ocimene	A.S	0.385
20.849	2,4,6-Octatriene, 2,6-dimethyl-, (E, Z)-	A.S	0.066
22.166	(Z)-4-Ethyl-3-nonen-5-yne	R.C	0.082
22.485	Benzenepropanal	R.C	0.071
25.220	Benzene, (2-propynyloxy)-	R.C	0.245
29.297	Cinnamaldehyde, (E)-	R.C	55.745
29.859	2-Methoxy-4-vinylphenol	A.S	0.608
33.734	1H-3a, 7-Methanoazulene, octahydro-3,8,8-trimethyl-6-methylene-, (3R,3aS,7S,8aS)-MSDS	R.C	0.157
34.648	Bicyclo[4.4.0]dec-1-ene, 2-isopropyl-5-methyl-9-methy lene-	R.C	0.092
35.009	3-Methylenecycloheptene	R.C	0.102
35.454	Alloaromadendrene	A.S	0.080
36.360	Spiro[5.5]undec-2-ene, 3,7,7-trimethyl-11-methylene-, (-)-	R.C	0.053
36.813	Naphthalene, 1,2,3,5,6,7,8,8a-octahydro-1,8a-dimethyl -7-(1-methylethenyl)-, [1S-(1.alpha.,7.alpha.,8a.alpha.)]-	R.C	0.041
37.618	Bicyclo[3.1.0]hexane, 6-isopropylidene-1-methyl	A.S	0.151
38.532	1H-Benzocycloheptene, 2,4a, 5,6,7,8-hexahydro-3,5,5,9-tetramethyl-, (R)-	A.S	0.060
40.219	(-)-Spathulenol	A.S	0.080
43.255	Methanone, (4-phenoxy-6-phenyl-1,2,5-dioxazinan-2-yl) phenyl	R.C	0.318
43.842	1 (3H)-Isobenzofuranone, 3-butylidene	A.S	1.217
47.164	trans-ligustilide	A.S	36.227
48.196	trans-ligustilide	A.S	0.383
48.599	Dibutyl phthalate	R.C	1.923
53.607	9,12-Octadecadienoic acid (Z, Z)-	R.C	0.204
59.328	Benzene, 1-(1-buten-3-yl)-2-vinyl	R.C	0.385
61.232	9-Octadecenamide, (Z)-	R.C	0.255
76.030	cis-ligustilide	A.S	0.156
77.691	β-tocopherol	R.C	0.202
83.487	β-sitosterol	R.C	0.293

(*R.C and A.S refer to *Rimulus cinnamon* and *Angelica sinenis*, respectively.)

Table 2: The influence of SA and $CaCl_2$ solution concentration on DL (%) and EE (%) of microcapsules (mean±SD, *n*=3)

Sample Code	Concentration of SA (%)	Concentration of $CaCl_2$ (%)	Concentration of CS (%)	DL (%)	EE (%)
R1	0.5	1.0	2.0	12.21±0.03	61.49±0.04
R2	1.0	1.0	2.0	22.60±0.02	72.55±0.04
R3	1.5	1.0	2.0	15.34±0.16	66.27±0.26

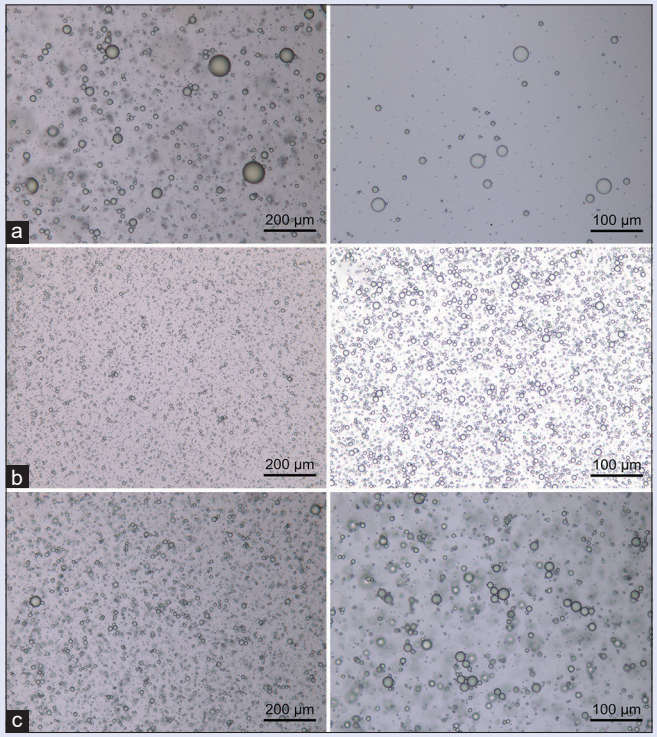

Figure 2: Optical micrographs of the CVOs emulsion prepared with (a) 0.5% SA, (b) 1.0% SA, and (c) 1.5% SA

enough, the oil in the droplets can be squeezed out during or after the alginate-calcium cross-linking due to the internal stress exerted on the microcapsules,[37,38] forming fractured or cracked microcapsules. Reportedly, increasing $CaCl_2$ concentration will result in the diffusion of more Ca^{2+} into the alginate beads, and the drug displaced by these ions will cause a decrease in EE%.[39] Therefore, the $CaCl_2$ concentration finally selected here is 1.0%.

Calcium alginate gels with a cross-linked network structure can complex with CS molecules to finally form microcapsules with mechanical strength and elasticity. The CS concentration mainly affects microcapsule formability, capsule wall strength, and sustained release performance.[40] With the increase of CS concentration in a certain range, the microcapsule mold ability and capsule wall mechanical strength, as well as the sustained release performance, are strengthened.[41] In the research above, when the concentration is low (1.0%), the polyelectrolyte membranes as formed are thin, resulting in low mechanical strength of the microcapsule wall. When the CS concentration is 1.5% to 2.0%, spherical microcapsules with high strength and regular capsule wall shape are formed, and the sustained release performance of the microcapsules is continuously enhanced. The microcapsules stick together and can hardly disperse because of the viscosity of the 3.0% CS is too high. The charge density of CS molecules is increased sharply, leading to the extension of molecular space and further to weakened molecular diffusion and lower cross-linking degree with alginate. The microcapsule density and membrane strength are both low.[42] Therefore, the CS concentration selected finally is 2.0%. Consequently, the selected concentrations are as follows: 1.0% SA, 2.0% CS, and 1.0% $CaCl_2$.

When we previously used the Soxhlet extractor to extract CVOs,[43] the results of DL (%) are consistent with the evaluation results of cinnamaldehyde. Results confirm that cinnamaldehyde can be used to evaluate DL (%) and EE (%).

Characterization of CVOs microcapsule

SEM analysis

SEM images of CVOs microcapsules in Figure 3 showed that the microcapsules were adhesive with each other and part of the particles are aggregated with spherical shape, slight dents, cracks, and had a relatively smooth surface, which may be caused by the uneven shrinkage of the capsule material during the vacuum drying process. These may demonstrate that the microcapsules were successfully prepared and stable through the preparation and drying process.

FT-IR analysis

The FT-IR spectra of SA, CS, CVOs, CVOs microcapsules, physical mixtures, and blank microcapsules were obtained. SA [Figure 4E] has typical absorption bands at 3428.40 cm^{-1} (O-H stretching vibration), 2162.72 cm^{-1} (C-O stretching vibration), 1614.57 cm^{-1} (-COO- asymmetric stretching vibration), 2974.66 cm^{-1}, and 2931.31 cm^{-1} corresponding to C-H stretching vibration. The characteristic absorption band of CS [Figure 4D] is observed at 3426.32 cm^{-1} (N-H stretching vibration), 1650.27 cm^{-1} (N-H bending vibration), 2884.16 cm^{-1} (C-H stretching vibration), 1156.23 cm^{-1} (C-N stretching vibration), and 1049.57 cm^{-1} (C-O-C asymmetric stretching vibration). CVOs [Figure 4B] has typical absorption bands at 3503.33 cm^{-1} and 3337.84 cm^{-1} (hydroxyl O-H stretching vibration), 2929.61 cm^{-1} (methylene C-H antisymmetric stretching vibration), 1762.79 cm^{-1} (C = O stretching vibration), and 1626.29 cm^{-1} (O-H bending vibration). In the infrared spectra of the blank microcapsules [Figure 4C], the -COO- characteristic absorption band near 1600 cm^{-1} and 1400 cm^{-1} of SA and the N-H characteristic absorption band near 1650 cm^{-1} of CS were significantly weakened, and the band disappeared at 1000 cm^{-1}, indicating that SA reacted with CS. In the infrared spectrum of the physical mixture [Figure 4A], the characteristic absorption band of CVOs, SA, and CS all existed and did not decrease, indicating that only a simple mechanical mixing operation was carried out without reaction. In the infrared spectrum of CVOs microcapsule [Figure 4F], the characteristic absorption band of CVOs was retained, the stretching vibration peak of ester carbonyl C = O at 1768.16 cm^{-1} was retained, while the absorption peak intensity at 1606.42 cm^{-1} and 1450.45 cm^{-1} and the absorption peak intensity below 1300 cm^{-1} were also greatly weakened.

X-ray diffraction (XRD)

The crystalline structures of CS, the physical mixture, SA, microcapsules, and blank microcapsules were investigated by XRD [Figure 5].

CS shows a characteristic crystalline peak at $2\theta = 20°$, while both the microcapsules and blank microcapsules display a broader and weaker peak indicative of a reduced crystallinity at $2\theta = 21.5°$, suggesting that

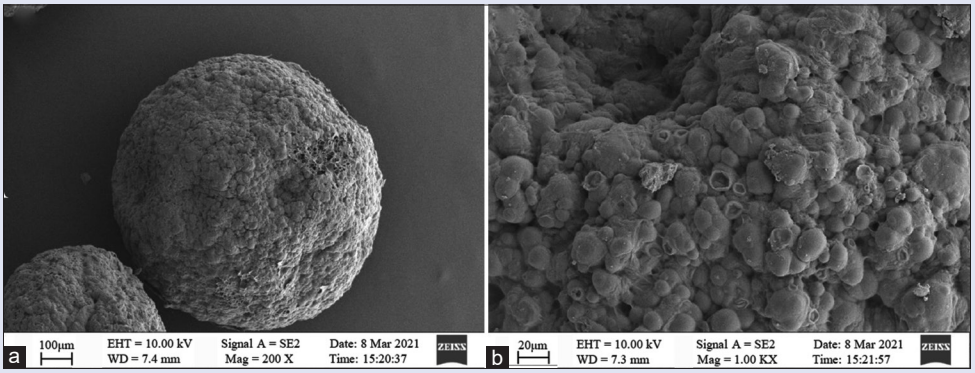

Figure 3: SEM micrographs of CVOs microcapsules obtained under the optimal preparation conditions. (a) magnification 200×; (b) magnification 1,000×

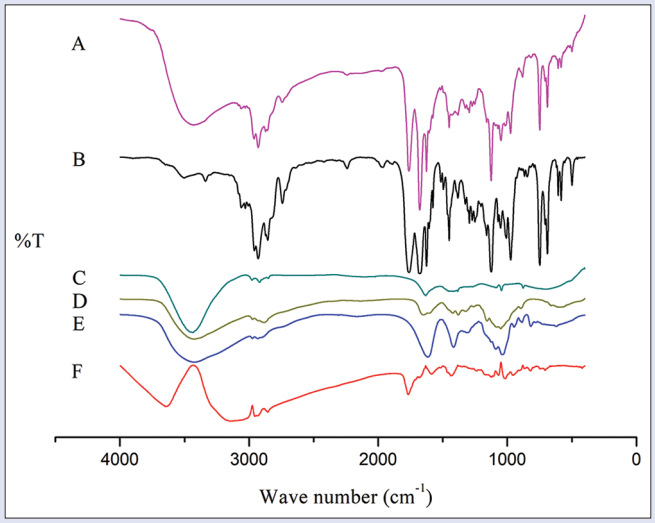

Figure 4: Infrared spectra of (A) Physical mixtures, (B) CVOs, (C) Blank microcapsules, (D) CS, (E) SA, and (F) Microcapsules

the introduction of SA onto CS will cause a remarkable decrease in crystallinity.[44] The physical mixture has a broad diffraction peak at about 20°, which is a superposition of the diffraction peaks of SA, CS, and the CVOs. There are still crystal diffraction peaks of each substance in the physical mixture, indicating that only mechanical mixing rather than chemical reaction has occurred between CS and SA.

Thermogravimetric (TG) analysis

TG analysis was used to assess the thermal stability of the microcapsules and determine pyrolysis the temperature and pyrolysis rate, which are useful for evaluating the thermal stability of different macromolecules. The thermal properties of the SA/CS wall and CVOs microcapsules were investigated by TG [Figure 6]. The TG curves of the SA/CS wall and microcapsules both show three steps of weight loss. A small loss related to water removal exists below 200°C in the two curves. For the SA/CS wall, weight losses appear in the ranges of 200°C to 300°C and 300°C to 500°C, which can be ascribed to the dehydration and the decomposition of CS and SA. The curve of the microcapsules shows a sharp weight decrease at 200°C, which is attributed to the degradation of the encapsulated CVOs, indicating that the microcapsules possess strong heat resistance.

Determination of swelling property

The microcapsules were placed in SGF(pH 1.2), NS(pH 7.0), and SIF (pH 8.0) to analyze their swelling conditions under different pH [Figure 7].

The swelling property of the microcapsules was the least in the SGF. After 120 min, the particle size of the microcapsules did not significantly change, and the swelling ratio was 1.0473 ± 0.01, which was only slight swelling and indicated that the microcapsules were relatively stable in the SGF. At 20 min, the swelling ratio was 0.9668 and the main reason was that the CS shell was dissolved in the acidic solution. Therefore, when the CS shell was dissolved, the particle size of the microcapsules decreased. The microcapsules swelled at a constant rate in NS, and the swelling ratio was 1.7486 ± 0.03 after 120 min, suggesting no rupture occurred. In the SIF, the swelling rate of microcapsules was the highest. After 40 to 60 min, the microcapsules floated on the solution and some even swelled and broke. After 120 min, the swelling ratio increased to 2.4674 ± 0.07. The swelling properties of the microcapsules in different media can reflect the pH responsiveness of the microcapsules.

When the medium pH increased from 1.2 to 8.0, the swelling ratio of the microcapsules rose from 1.05 to 2.46, indicating that the swelling ability of microcapsules was enhanced with the rise of the medium pH.[45] This is because the hydrogen bonding between the -COOH of the polymer chain and the solvent molecules results in a shrinkage of the network structure at pH 1.2, reducing the swelling behavior. At pH 7.0, the amino groups are still protonated -NH^{3+} and therefore electrostatically interact with the ionized carboxyl groups (-COO-) of alginate, forming a CS-SA complex polyelectrolyte structure that inhibits intrusion of water molecules into the microcapsules.[46] The reason for the increase in swelling ratio at pH 8.0 is because the -COOH of SA is all converted to -COO- and the existence of ion-ion repulsion leads to the repulsion of water molecules.[47] In this pH range, the carboxyl groups of uronic acids are completely ionized, which allows for the rapid intrusion of water molecules into the CVOs microcapsules, thus leading to an extremely high swelling degree.[48]

In vitro dissolution experiment

SGF, NS, and SIF were used to investigate the release performance of microcapsules with different pHs. The volume of the release medium can ensure the sink conditions for the release of cinnamaldehyde. When released under acidic conditions, CS in the outer layer and middle layer of the composite membrane of the microcapsules swelled. When alginate and its calcium salt shrank, the dispersed drug was diffused into the acidic medium through the pores left by CS swelling. When released in an alkaline buffer solution, alginate and its calcium salt were dissolved, and the cross-linked CS formed a network membrane skeleton structure, which was driven by the difference between inside and outside drug concentrations. Noticeably, the cumulative release rate of drugs in the SGF was significantly higher than those in the NS and SIF in the first 1 h [Figure 8a]. This may be because the cationic

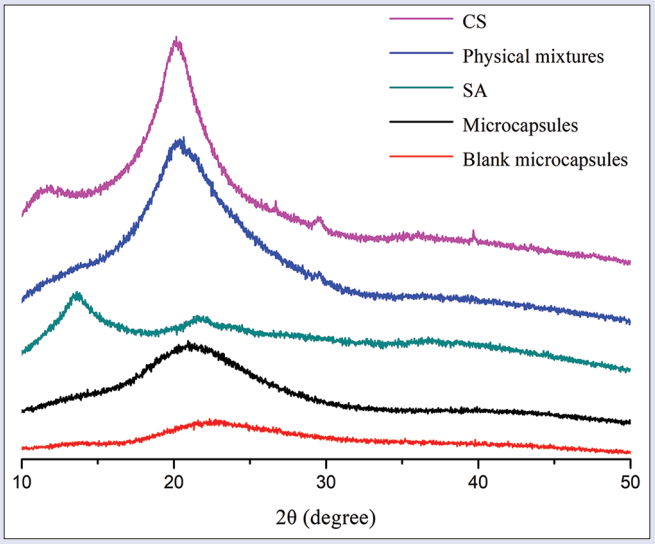

Figure 5: XRD patterns of CS, Physical mixtures, SA, microcapsules, and Blank microcapsules

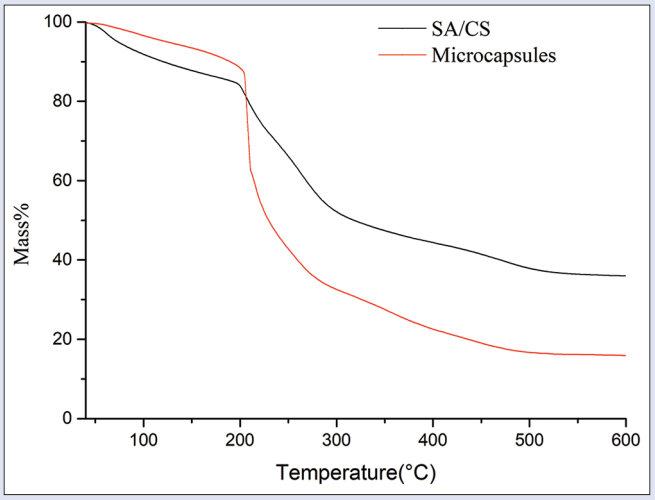

Figure 6: TG spectra of SA/CS wall and microcapsules

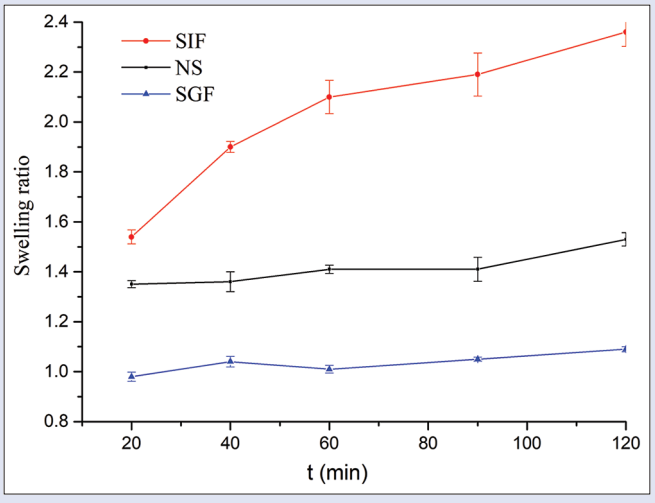

Figure 7: Swelling profiles of CVOs microcapsule at SGF (pH 1.2), NS, and SIF (pH 6.8)

polymer CS in the outer layer of the microcapsules electrostatically combined with the anionic substances in the volatile oil. In the acidic medium, CS absorbed water and swelled, thereby destroying the salt bond. However, the amino group of CS in the weakly alkaline medium was still tightly bound to the negatively charged group of the anionic substance in the volatile oil, so the drug release rate of the microcapsules was slower than in the acidic medium.[49,50] The release behaviors of the physical mixtures were similar among the three media [Figure 8b, c, and d]. The cumulative release rate of the physical mixture was slower than that of the microcapsules in any of the three media, which may be due to the low solubility of CVOs in the three media.

The release of microcapsules was a non-steady-state process. The main stage of controlled release was the diffusion of the capsule core from the capsule wall, and its main diffusion resistance came from the density of the membrane layer formed by the microcapsule wall material. The drug was dissolved or dispersed in the polymer, the release of cinnamaldehyde was fast and then slows, and the cinnamaldehyde adsorbed on the outer layer and surface of the microcapsules was released at the beginning. When the solvent diffused into the polymer, the polymer began to swell, then the polymer chain relaxed, and the drug was diffused out. The *in vitro* release curves of the CVO microcapsules were linearly fitted under three dissolution medium conditions. A zero-order model, a first-order model, the Higuchi model, and the Ritger-Peppas model were used to comparatively fit the correlation coefficient r^2.[51] According to the fitting results in Table 3, the *in vitro* drug release curves of the CVOs microcapsules in different dissolution media were the best fitted by the first-order model. In the SGF, NS, and SIF, the results of r^2 in fitting between the *in vitro* release curve and the first-order model are 0.9967, 0.9657, and 0.9447, respectively, indicating that the first-order model can best describe the situation of drug release *in vitro*.

Storage stability

Improving storage stability is important for the storage and transportation of unstable, volatile, and oxidizable drugs. As shown in Figure 9, the DL (%) of the physical mixture was sharply reduced during 30 days. The DL (%) reduction rate of the microcapsules was low, which suggested high stability. These results prove that the microencapsulated CVOs have high storage stability, which is conducive to storage and transportation.

Table 3: Fitting equation of *in vitro* release of CVOs microcapsules in SGF, NS, and SIF dissolution medium

Release media	Fitted Model	Fitted equation	r^2
SGF	Zero-order	Qt=51.5491+0.1225t	0.4882
	First-order	ln (1-Q_t) = 0.02701t	0.9967
	Higuchi	Qt=33.1368+3.2710$t^{1/2}$	0.6971
	Ritger-Peppas	Qt=21.8845$t^{0.2448}$	0.8030
NS	Zero-order	Qt=36.9846+0.1885t	0.5406
	First-order	ln (1-Q_t) = 0.01483t	0.9657
	Higuchi	Qt=9.3326+4.9677$t^{1/2}$	0.7445
	Ritger-Peppas	Qt=10.1885$t^{0.3874}$	0.7812
SIF	Zero-order	Qt=37.5192+0.2004t	0.5137
	First-order	ln (1-Q_t) = 0.01466t	0.9447
	Higuchi	Qt=7.7930+5.3130$t^{1/2}$	0.7192
	Ritger-Peppas	Qt=10.0890$t^{0.3967}$	0.7523

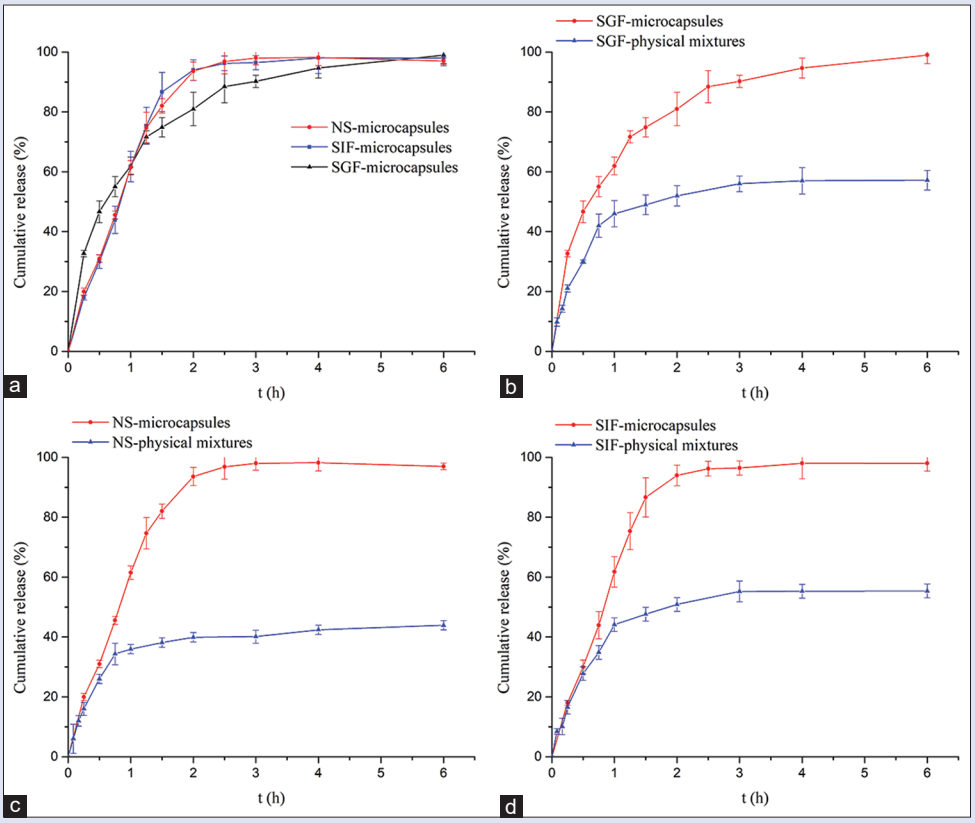

Figure 8: Cumulative release curve of CVOs microcapsules and physical mixtures at SGF (pH 1.2), NS, and SIF (pH 6.8)

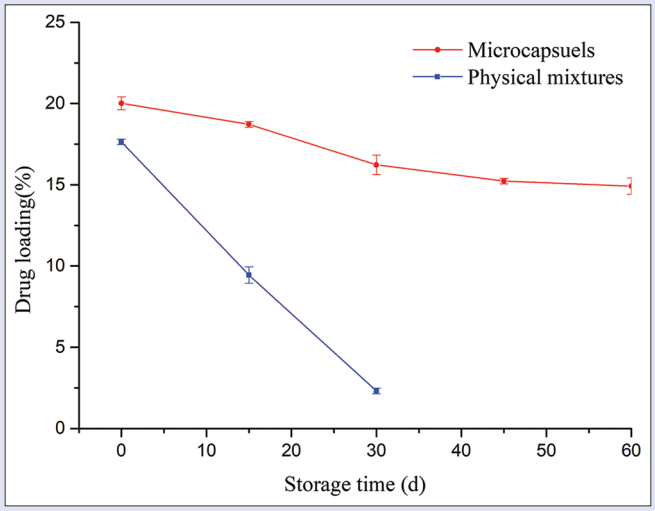

Figure 9: The storage stability of microcapsules and physical mixtures

CONCLUSION

In this study, SA and CS were selected as capsule materials to study the microencapsulation of CVOs, the factors of microcapsule formation were investigated, and the appearance, DL performance, and stability of the microcapsules were evaluated. The result showed that SA and CS can efficiently encapsulate CVOs with excellent morphology, DL (%), EE (%), and stability. Therefore, successful microencapsulation will expand the application of CVOs and increase the utilization rate. In subsequent applications, this stable carrier will facilitate the application of many preparations, such as tablets and capsules.

Acknowledgements

The authors appreciate the support of Guangzhou Baiyunshan Huangpu Hutchison Co., Ltd.

Financial support and sponsorship

This work was financially supported by the Guangzhou Science and Technology Plan Project (number 201904010112) and the "Yang Fan Plan" team project of Guangdong Province (No. 2017YT05S137).

Conflicts of interest

There are no conflicts of interest.

REFERENCES

1. Xu F, Sang W, Li L, He X, Wang F, Wen T, *et al.* Protective effects of ethyl acetate extracts of *Rimulus cinnamon* on systemic inflammation and lung injury in endotoxin-poisoned mice. Drug Chem Toxicol 2019;42:309-16.
2. Li X, Lu HY, Jiang XW, Yang Y, Xing B, Yao D, *et al.* Cinnamomum cassia extract promotes thermogenesis during exposure to cold via activation of brown adipose tissue. J Ethnopharmacol 2021;266:113413. doi: 10.1016/j.jep. 2020.113413.
3. Sadeghi S, Davoodvandi A, Pourhanifeh MH, Sharifi N, ArefNezhad R, Sahebnasagh R, *et al.* Anti-cancer effects of cinnamon: Insights into its apoptosis effects. Eur J Med Chem 2019;178:131-40.
4. Jin Y, Qu C, Tang YP, Pang HQ, Liu LL, Zhu ZH, *et al.* Herb pairs containing *Angelicae Sinensis* Radix (Danggui): A review of bio-active constituents and compatibility effects. J Ethnopharmacol 2016;181:158-71.
5. Luo C, Chen Q, Liu B, Wang S, Yu H, Guan X, *et al.* The extracts of Angelica sinensis and *Cinnamomum cassia* from Oriental medicinal foods regulate inflammatory and

autophagic pathways against neural injury after ischemic stroke. Oxid Med Cell Longev 2021;2021:9663208. doi: 10.1155/2021/9663208.

6. Cheng B, Zheng H, Wu F, Wu JX, Liu XW, Tang CL, *et al.* Metabolomics analysis of danggui sini decoction on treatment of collagen-induced arthritis in rats. J Chromatogr B Analyt Technol Biomed Life Sci 2017;1061-1062:282-91.
7. Shi MY, Li JL, Xie Y, Yang S, Jian X, Wang LJ. Optimization of preparation technology of β-cyclodextrin inclusion complexes for volatile oil in Guanxinkang capsule. Chin J Exp Tradit Med Formulae 2013;19:47-50.
8. Chen J, Chen WH, Wang R, Shi YP. Study on β-cyclodextrin inclusion technology of volatile oil from Yukui capsule. Chin J Exp Tradit Med Formulae 2011;17:19-22.
9. Liu M, Qiang QH, Ling Q, Yu CX, Li X, Liu S, *et al.* Effects of Danggui Sini decoction on neuropathic pain: Experimental studies and clinical pharmacological significance of inhibiting glial activation and proinflammatory cytokines in the spinal cord. Int J Clin Pharmacol Ther 2017;55:453-64.
10. Li MT, Li CG, Zhou Y, Tian H, Deng QY, Liu HF, *et al.* Optimization of cinnamaldehyde microcapsule wall materials by experimental and quantitative methods. J Appl Polym Sci 2021;138:212-20.
11. Li C, Chen W, Siva S, Cui H, Lin L. Electrospun phospholipid nanofibers encapsulated with cinnamaldehyde/HP-β-CD inclusion complex as a novel food packaging material. Food Packag Shelf Life 2021;28:100647. doi: 10.1016/j.fpsl. 2021.100647.
12. Li FF, Wang HF, Mei XH. Preparation and characterization of phytosterol-loaded microcapsules based on the complex coacervation. J Food Eng 2021;311:110718-24.
13. Muhoza B, Xia SQ, Cai JB, Zhang X, Duhoranimana E, Su J. Gelatin and pectin complex coacervates as carriers for cinnamaldehyde: Effect of pectin esterification degree on coacervate formation, and enhanced thermal stability. Food Hydrocoll 2019;87:712-22.
14. Martins E, Poncelet D, Rodrigues RC, Renard D. Oil encapsulation techniques using alginate as encapsulating agent: Applications and drawbacks. J Microencapsul 2017;34:754-71.
15. Hui PC, Wang WY, Kan CW, Ng FS, Zhou CE, Wat E, *et al.* Preparation and characterization of chitosan/sodium alginate (CSA) microcapsule containing cortex moutan. Colloids Surf 2013;434:95-101.
16. Faidi A, Lassoued MA, Becheikh MEH, Touati M, Stumbé JF, Farhat F. Application of sodium alginate extracted from a Tunisian brown algae Padina pavonica for essential oil encapsulation: Microspheres preparation, characterization and *in vitro* release study. Int J Biol Macromol 2019;136:386-94.
17. Shamekhi F, Tamjid E, Khajeh K. Development of chitosan coated calcium-alginate nanocapsules for oral delivery of liraglutide to diabetic patients. Int J Biol Macromol 2018;120:460-7.
18. Maqbool M, Sadaf S, Bhatti HN, Rehmat S, Kausar A, Alissa SA, *et al.* Sodium alginate and polypyrrole composites with algal dead biomass for the adsorption of Congo red dye: Kinetics, thermodynamics and desorption studies. Surf Interfaces 2021;25. doi: 10.1016/j.surfin. 2021.101183.
19. Zhao XL, Wang XJ, Lou T. Preparation of fibrous chitosan/sodium alginate composite foams for the adsorption of cationic and anionic dyes. J Hazard Mater 2021;403:124054. doi: 10.1016/j.jhazmat. 2020.124054.
20. Murguía-Flores DA, Bonilla-Ríos J, Canales-Fiscal MR, Sánchez-Fernández A. Protein adsorption through chitosan-alginate membranes for potential applications. Chem Cent J. 2016;10:26.
21. Li N, Zhang ZJ, Li XJ, Li HZ, Cui LX, He DL. Microcapsules biologically prepared using Perilla frutescens (l.) britt. essential oil and their use for extension of fruit shelf life. J Sci Food Agric 2018;98:1033-41.
22. Sy Piecco KWE, Aboelenen AM, Pyle JR, Vicente JR, Gautam D, Chen J. Kinetic model under light-limited condition for photoinitiated thiol-ene coupling reactions. ACS Omega 2018;3:14327-32.
23. Lotfy VF, Basta AH. Optimizing the chitosan-cellulose based drug delivery system for controlling the ciprofloxacin release versus organic/inorganic crosslinker, characterization and kinetic study. Int J Biol Macromol 2020;165:1496-506.
24. Shen L, Chen J, Bai Y, Ma Z, Huang J, Feng W. Physical properties and stabilization of microcapsules containing thyme oil by complex coacervation. J Food Sci 2016;81:N2258-62.
25. Mu HY, Song ZX, Wang X, Wang DD, Zheng XQ, Li XD. Microencapsulation of algae oil by complex coacervation of chitosan and modified starch: Characterization and oxidative stability. Int J Biol Macromol 2022;194:66-73.
26. Nayak S, Dey S, Kundu SC. Silk sericin-alginate-chitosan microcapsules: Hepatocytes encapsulation for enhanced cellular functions. Int J Biol Macromol 2014;65:258-66.
27. Chaib S, Benali N, Arhab R, Sadraoui Ajmi IS, Bendaoued H, Romdhane M. Preparation of thymus vulgaris essential oil microcapsules by complex coacervation and direct emulsion: Synthesis, characterization and controlled release properties. Arab J Sci Eng 2021;46:5429-46.
28. Li L, Song WL, Shen CH, Dong QF, Wang YF, Zuo S. Active packaging film containing oregano essential oil microcapsules and their application for strawberry preservation. J Food Process Preserv 2020;44:154-86.
29. Zam W, Bashour G, Abdelwahed W, Khayata W. Alginate-pomegranate peels' polyphenols beads: Effects of formulation parameters on loading efficiency. Braz J Pharm Sci 2014;50:741-8.
30. Ortiz M, Jornada DS, Pohlmann AR, Guterres SS. Development of novel chitosan microcapsules for pulmonary delivery of dapsone: Characterization, aerosol performance, and *in vivo* toxicity evaluation. AAPS PharmSciTech 2015;16:1033-40.
31. Dima C, Pătraşcu L, Cantaragiu A, Alexe P, Dima Ş. The kinetics of the swelling process and the release mechanisms of Coriandrum sativum L. essential oil from chitosan/alginate/inulin microcapsules. Food Chem 2016;195:39-48.
32. Mankala SK, Korla AC, Gade S. Development and evaluation of aceclofenac-loaded mucoadhesive microcapsules. J Adv Pharm Technol Res 2011;2:245-54.
33. Noppakundilograt S, Piboon P, Graisuwan W, Nuisin R, Kiatkamjornwong S. Encapsulated eucalyptus oil in ionically cross-linked alginate microcapsules and its controlled release. Carbohydr Polym 2015;131:23-33.
34. Abbaspourrad A, Datta SS, Weitz DA. Controlling release from pH-responsive microcapsules. Langmuir 2013;29:12697-702.
35. Kaygusuz H, Erim FB, Pekcan O, Akın Evingür GA. Cation effect on slow release from alginate beads: A fluorescence study. J Fluoresc 2014;24:161-7.
36. Zhang YL, Wei W, Lv PP, Wang LY, Ma GH. Preparation and evaluation of alginate-chitosan microspheres for oral delivery of insulin. Eur J Pharm Biopharm 2011;77:11-9.
37. Celli GB, Ghanem A, Brooks MSL. Optimized encapsulation of anthocyanin-rich extract from haskap berries (Lonicera caerulea L.) in calcium-alginate microparticles. J Berry Res 2015;6:1-11.
38. Natrajan D, Srinivasan S, Sundar K, Ravindran A. Formulation of essential oil-loaded chitosan-alginate nanocapsules. J Food Drug Anal 2015;23:560-8.
39. Halder A, Maiti S, Sa B. Entrapment efficiency and release characteristics of polyethyleneimine-treated or -untreated calcium alginate beads loaded with propranolol-resin complex. Int J Pharm 2005;302:84-94.
40. He HZ, Hong Y, Gu ZB, Liu GD, Cheng L, Li Z. Improved stability and controlled release of CLA with spray-dried microcapsules of OSA-modified starch and xanthan gum. Carbohydr Polym 2016;147:243-50.
41. Singh B, Chauhan D. Barium ions crosslinked alginate and sterculia gum-based gastroretentive floating drug delivery system for use in peptic ulcers. Int J Polym Mater 2011;60:684-705.
42. Jayanudin, Fahrurrozi M, Wirawan SK, Rochmadi. Preparation of chitosan microcapsules containing red ginger oleoresin using emulsion crosslinking method. J Appl Biomater Funct Mater 2019;17:2280800018809917. doi: 10.1177/2280800018809917.
43. Aidi Wannes W, Mhamdi B, Sriti J, Ben Jemia M, Ouchikh O, Hamdaoui G, *et al.* Antioxidant activities of the essential oils and methanol extracts from myrtle (Myrtus communis var. italica L.) leaf, stem and flower. Food Chem Toxicol 2010;48:1362-70.
44. Wang Y, Tan C, Davachi SM, Li P, Davidowsky P, Yan B. Development of microcapsules using chitosan and alginate via W/O emulsion for the protection of hydrophilic compounds by comparing with hydrogel beads. Int J Biol Macromol 2021;177:92-9.
45. Liu YH, Liu MY, Zhao J, Wang D, Zhang L, Wang H, *et al.* Microencapsulation of Osmanthus essential oil by interfacial polymerization: Optimization, characterization, release kinetics, and storage stability of essential oil from microcapsules. J Food Sci 2021;86:5397-408.
46. Li Y, McClements DJ. Controlling lipid digestion by encapsulation of protein-stabilized lipid droplets within alginate-chitosan complex coacervates. Food Hydrocoll 2011;25:1025-33.
47. Thuekeaw S, Angkanaporn K, Chirachanchai S, Nuengjamnong C. Dual pH responsive via double – layered microencapsulation for controlled release of active ingredients in simulated gastrointestinal tract: A model case of chitosan-alginate microcapsules containing basil oil (Ocimum basilicum Linn.). Polym Degrad Stab 2021;191. doi: 10.1016/j.polymdegradstab. 2021.109660.
48. Čalija B, Cekić N, Savić S, Daniels R, Marković B, Milić J. pH-sensitive microparticles for oral drug delivery based on alginate/oligochitosan/Eudragit(®) L100-55 "sandwich" polyelectrolyte complex. Colloids Surf B Biointerfaces 2013;110:395-402.

49. Khodabakhsh Aghdam SK, Khoshfetrat AB, Rahbarghazi R, Jafarizadeh-Malmiri H, Khaksar M. Collagen modulates functional activity of hepatic cells inside alginate-galactosylated chitosan hydrogel microcapsules. Int J Biol Macromol 2020;156:1270-8.
50. Ge XH, Du YH, Huang XL, Mo LJ, Wang HX, Qiu T. The preparation of peppermint oil/2-hydroxypropyl-β-cyclodextrin/chitosan composite microcapsule and their prolonged retaining ability. Microfluid Nanofluid 2021;25:1-13.
51. Wang T, Chen KR, Zhang XZ, Yu Y, Yu D, Jiang L, *et al.* Effect of ultrasound on the preparation of soy protein isolate-maltodextrin embedded hemp seed oil microcapsules and the establishment of oxidation kinetics models. Ultrason Sonochem 2021;77:105700. doi: 10.1016/j.ultsonch. 2021.105700.